technologies

MDPI

Article

High-Efficiency Broadband Doherty Power Amplifier Optimization Based on Genetic Algorithms and Neural Networks

Jianping Xing, Yicheng Cai, Yixian Xu, Weiqing Dong and Jing Xia *

School of Computer Science and Communication Engineering, Jiangsu University, Zhenjiang 212013, China; 3220601044@stmail.ujs.edu.cn (J.X.); 3220601040@stmail.ujs.edu.cn (Y.C.); 3220601043@stmail.ujs.edu.cn (Y.X.); 1000002864@ujs.edu.cn (W.D.)

* Correspondence: jingxia@ujs.edu.cn

Abstract

This paper proposes a design method for high-efficiency broadband Doherty power amplifiers (DPAs) optimized through a co-simulation approach combining genetic algorithms and neural networks. The method integrates the global search capability of genetic algorithms with the predictive power of neural networks to efficiently optimize the DPA matching network parameters. Key performance metrics such as output power, efficiency, and gain are incorporated into the objective function for comprehensive optimization. A DPA operating from 1.5 GHz to 2.6 GHz was designed and fabricated. Measurement results demonstrate that the optimized amplifier achieves saturated output power between 42.19 dBm and 44.7 dBm, saturated efficiency from 51.4% to 61.8%, and 6 dB back-off efficiency ranging from 44.3% to 56.4% across the bandwidth. These results verify the feasibility and effectiveness of the proposed optimization method.

Keywords: genetic algorithm; neural network; high efficiency; broadband; Doherty power amplifier

check for updates

Academic Editor: Valeri Mladenov

Received: 21 June 2025
Revised: 14 August 2025
Accepted: 18 August 2025
Published: 19 August 2025

Citation: Xing, J.; Cai, Y.; Xu, Y.; Dong, W.; Xia, J. High-Efficiency Broadband Doherty Power Amplifier Optimization Based on Genetic Algorithms and Neural Networks. *Technologies* **2025**, *13*, 371. https://doi.org/10.3390/technologies13080371

Copyright: © 2025 by the authors. Licensee MDPI, Basel, Switzerland. This article is an open access article distributed under the terms and conditions of the Creative Commons Attribution (CC BY) license (https://creativecommons.org/licenses/by/4.0/).

1. Introduction

With the rapid advancement of wireless communication technologies, power amplifiers (PAs) are increasingly expected to deliver both high efficiency and wide operational bandwidth [1]. Among various PA topologies, the Doherty power amplifier (DPA) has garnered significant attention due to its high efficiency, linearity, and bandwidth [2], making it a key enabler in modern communication systems.

To further enhance PA performance, various design methodologies have been proposed in recent years. Ref. [3] proposed a three-stage DPA incorporating impedance compensation in the load combiner, effectively extending the bandwidth. Ref. [4] introduced an improved load modulation network that significantly boosts back-off efficiency through optimized matching networks. Ref. [5] exploited the dual-band characteristics of T-shaped networks, enabling different load modulation paths at selected operating frequencies, thereby achieving high efficiency and output power. Ref. [6] designed a DPA based on a composite objective function constrained by both impedance and phase characteristics, improving efficiency consistency under power back-off conditions.

In addition, optimization algorithms and artificial intelligence techniques have been widely applied to PA design. In Refs. [7,8], Bayesian optimization was adopted to automate the design process, resulting in improved performance metrics. Refs. [9,10] applied

simulated annealing and particle swarm optimization to achieve efficient design of broadband and multi-band PAs. Ref. [11] employed multi-objective optimization techniques to address the challenges of broadband matching. Ref. [12] proposed a novel surrogate model-assisted hybrid optimization approach for efficient and general-purpose automatic PA design. Ref. [13] presented a deep learning-based inverse design method for broadband PAs, enabling effective broadband matching and power flatness optimization. Despite these advancements, achieving an optimal trade-off between efficiency and bandwidth continues to pose a significant challenge in PA design.

To address this issue, this paper presents a hybrid optimization method that integrates genetic algorithms and neural networks to optimize broadband DPA design. Genetic algorithms are well known for their robustness and strong global search capabilities in solving complex optimization problems. By performing global exploration of the design space [14], genetic algorithms have become a powerful tool for handling nonlinear, high-dimensional design tasks. On the other hand, neural networks, with their adaptive learning ability and nonlinear modeling capacity [15], can accurately predict the performance of power amplifiers under varying circuit parameters. The integration of these two techniques forms an efficient collaborative optimization framework, effectively improving both the efficiency and bandwidth in broadband power amplifier design.

The remainder of this paper is organized as follows. Section 2 introduces the proposed optimization framework. Section 3 presents the detailed design methodology and implementation process. Section 4 discusses the experimental setup and measurement results. Section 5 concludes the paper.

2. Genetic Algorithm and Neural Network

In the field of optimization, the integration of Genetic Algorithms and Neural Networks has become an effective approach for solving complex optimization problems. For examples, Refs. [16,17] dynamically combined multi-objective genetic algorithms (MOGAs) with neural networks to tackle intricate optimization tasks in the physical sciences. The proposed DNMOGA algorithm incorporates enhancements such as dynamic reallocation of evaluation resources across individuals, enabling it to handle stringent constraints and preference structures inherent in physical optimization problems. This approach was successfully applied to optimize the shape of superconducting radio-frequency (SRF) cavities, yielding designs that outperformed those obtained through manual tuning. By combining the global search capabilities of GAs with the rapid evaluation and modeling efficiency of NNs, this hybrid method significantly enhances both optimization accuracy and computational efficiency.

To address the limitations of traditional optimization techniques in broadband Doherty power amplifier (DPA) design, we propose a hybrid optimization framework that combines the global exploration capability of genetic algorithms (GAs) with the predictive efficiency of neural networks (NNs). This integration significantly improves the computational speed while maintaining optimization accuracy.

1. Overview of the Hybrid Optimization Framework

The theoretical foundation and implementation process of this combined approach are detailed as follows.

In the implementation, the initial population is generated using Latin Hypercube Sampling (LHS), a neural network model is constructed and trained, a dynamic mutation strategy and crossover operations are employed to generate new individuals, and an elitism strategy is applied to update the population. Finally, the accuracy of the optimization results is ensured by validating the true fitness of the best solution. The pseudo-code of the algorithm is presented in Algorithm 1.

Algorithm 1: The Complete Optimization Process

Input: Maximum number of generations; Population size;
Output: Best solution and fitness;

1. Initialize environment and parameters;
2. Generate initial population using LHS;
3. Define neural network (NN) architecture;
4. Set NN training options;
5. Initialize historical data storage;
6. Compute initial fitness values for the population;
7. **for** each generation from 1 to max_generations **do**
8. Train NN using current population and historical data;
9. Generate offspring through crossover, mutation;
10. Perform partial real evaluation using NN prediction;
11. Execute environmental selection to update parent population;
12. Recompute fitness for predicted individuals;
13. Identify the best individual and fitness of current generation;
14. Update historical population and fitness data;
15. **end for**

Step 1: Initial Population Generation.

To ensure uniform distribution of the initial population across each dimension [18], Latin Hypercube Sampling (LHS) is employed. LHS is a statistical sampling technique that divides the interval $[L_d, U_d]$ of each input variable dimension into N subintervals and randomly selects one sample point x from each subinterval. This method guarantees uniform coverage of the sample space in every dimension and avoids sample clustering or sparsity issues caused by random sampling, thereby improving the quality of the initial population. For each sampled individual x, its fitness value $f(x)$ is computed and stored. The fitness function is the core of the optimization problem, evaluating the quality of each individual based on the objective criteria. The fitness values of the initial population provide the basis for subsequent optimization. In this study, all individuals are generated using a random number seed to ensure stochasticity.

Step 2: Neural Network Model Construction.

The neural network consists of an input layer, hidden layers, and an output layer [19]. The input layer receives the optimization parameters, while the output layer provides the corresponding performance metrics, such as objective function values. The hidden layers extract features from the input data and perform nonlinear transformations to enable the network to learn the complex relationships between inputs and outputs. The neural network model can be mathematically represented as

$$f(x) = \sigma(W_3 \cdot \sigma(W_2 \cdot \sigma(W_1 \cdot x + b_1) + b_2) + b_3) \quad (1)$$

where W_1, W_2, W_3 denote weight matrices, b_1, b_2, b_3 are bias vectors, and $\sigma(\cdot)$ is the activation function.

In this study, the input layer of the network receives optimization parameters, which are subsequently processed by a feature input layer. The hidden layers are composed of multiple components. Initially, there is a fully connected layer with 128 neurons, followed by a batch normalization layer, which facilitates the acceleration of network convergence and enhances the stability of the training process. Subsequently, a ReLU activation function is applied to introduce nonlinearity, thereby enabling the network to capture complex patterns. To further prevent overfitting, a dropout layer with a dropout rate of 0.3 is

incorporated into the network. Following this, the network includes a Long Short-Term Memory (LSTM) layer, which comprises 64 units and is configured to output sequences. After the LSTM layer, another fully connected layer with 64 neurons is employed, succeeded by a ReLU activation function layer and a dropout layer with a dropout rate of 0.2. The output layer of the network is composed of a single fully connected layer with a single neuron designed to generate the final predictive output.

Step 3: Neural Network Training.

The neural network is trained by minimizing the mean squared error (MSE) between the predicted and true values, which is defined as

$$f(W,b) = \frac{1}{N}\sum_{i=1}^{N}(y_i - f(x_i))^2 \tag{2}$$

where W and b are the model's weights and biases, N is the number of training samples, y_i is the true value of the *i-th* sample, and $f(x_i)$ is the predicted value.

During the training phase, the network parameters are optimized using the Adam algorithm to minimize MSE, with a maximum of 200 iterations, a mini-batch size of 128, and an initial learning rate of 0.001. To avoid premature cessation of training based on validation performance, an early stopping criterion with a patience of 20 epochs is included. Through this iterative optimization process, the neural network progressively acquires the mapping between inputs and outputs, thereby facilitating rapid and accurate predictions on novel input data following the completion of training.

Step 4: Genetic Algorithm Operators—Mutation and Crossover.

Mutation and crossover operations are key to generating new individuals in the genetic algorithm. Mutation introduces new genetic variations by randomly altering parts of individuals, maintaining population diversity and preventing premature convergence. A dynamic mutation strategy is adopted to adjust mutation strength according to the generation number g:

$$\sigma_g = \sigma_0 \cdot \left(1 - \frac{g}{G_{max}}\right) \tag{3}$$

where σ_0 is the initial mutation strength and G_{max} is the maximum number of generations. This dynamic adjustment allows larger mutations in the early stages to explore the search space broadly, while reducing mutation strength in later stages to refine the search locally, thereby improving optimization accuracy.

Crossover generates offspring by exchanging parts of two parent individuals. For parents p_1 and p_2, the offspring c in dimension d is computed as

$$c_d = \beta \cdot p_{1,d} + (1-\beta) \cdot p_{2,d} \tag{4}$$

where $\beta \in [0,1,1]$ is the crossover coefficient. This operation combines desirable traits from both parents to produce offspring with potentially better fitness, driving the population toward optimal solutions.

After crossover, offspring undergo mutation to further increase diversity. The mutated value c'_d in dimension d is expressed as

$$c'_d = c_d + \mathcal{N}\left(0, \sigma_g \cdot (U_d - L_d)\right) \tag{5}$$

where $\mathcal{N}$ is a Gaussian random variable. This Gaussian mutation adds random noise to each dimension of the offspring, enabling exploration of new regions in the search space and helping avoid local optima.

In genetic algorithms, the elitism strategy is commonly employed to preserve the individuals with the highest fitness values, ensuring the overall quality of the population. After merging the offspring and parent populations, the elitism strategy selects the top 10% individuals in terms of fitness from the current population P_g as the elite set $Elite_g$, which are directly carried over to the next generation. This strategy can be formulated as

$$Elite_g = \{x \in P_g \mid f(x) \leq f_\alpha\} \tag{6}$$

where f_α is the fitness threshold correspong to the minimum α quantile. By retaining the individuals with the highest fitness, elitism ensures that the population maintains a high quality throughout evolution, thereby improving optimization efficiency.

Step 5: Fitness Evaluation of Mutated Offspring.

The mutated offspring require fitness evaluation. Since direct computation of fitness can be computationally expensive, the trained neural network is used to predict the fitness values F' of the offspring. For individuals with predicted low fitness as well as for a subset of randomly sampled individuals, true fitness evaluations are performed and their fitness values are updated accordingly. In this study, 20% of the dataset is allocated for validation purposes. This partial real evaluation strategy significantly reduces computational cost while maintaining optimization accuracy.

Step 6: Environmental Selection and Population Update.

Environmental selection is conducted by sorting the combined current population and offspring according to fitness values, selecting the lowest fitness individuals to form the next generation. The data of the new generation are stored in a historical population used for subsequent neural network training. The update of the historical population provides more training samples for the neural network, thereby further improving prediction accuracy. As the optimization progresses, the historical population grows, enabling the neural network to better adapt to changes in the solution space and enhance optimization efficiency. In this study, the training process utilizes data from the most recent 10 generations. Following this, fitness predictions of individuals are recalculated to identify the current best individual and fitness.

Step 7: Termination Condition and Output.

The optimization process terminates when a preset maximum number of iterations is reached or when fitness convergence criteria are met. Upon termination, the true fitness of the best predicted solution is verified. If the predicted best fitness differs from the true value, a re-evaluation of the entire population is performed to identify the true best solution. Finally, the best individual and its fitness value are outputted as the solution to the optimization problem.

2. Algorithm Testing

The proposed algorithm is evaluated using three different types of benchmark test functions. The details of these test functions are listed in Table 1.

Table 1. Benchmark test functions.

Test Function	Range
$f_1(x) = \sum_{i=1}^{n} x_i^2$	$[-100, 100]$
$f_2(x) = \sum_{i=1}^{n} (\sum_{j-1}^{i} x_j)^2$	$[-100, 100]$
$f_3(x) = max\{\lvert x_i \rvert, 1 \leq i \leq n\}$	$[-100, 100]$

To guarantee the reliability of the surrogate model integrated within our Genetic Algorithm, we employ the Root Mean Squared Error (RMSE) as a principal metric to evaluate the accuracy of the Neural Network predictions relative to the actual fitness values. The RMSE provides a quantitative measure of the average magnitude of the errors between the predicted and actual fitness values. The RMSE is calculated as follows:

$$\text{RMSE} = \sqrt{\frac{1}{n}\sum_{i=1}^{n}(y_i - \hat{y}_i)^2} \tag{7}$$

where y_i represents the actual fitness value of the i -th individual, $\hat{y}_i$ is the predicted fitness value from the neural network, and n is the number of individuals used for validation.

In addition to RMSE, we calculate the coefficient of determination R^2 to evaluate the goodness-of-fit of the neural network predictions. The R^2 score indicates the proportion of variance in the actual fitness values that is predictable from the surrogate model:

$$R^2 = 1 - \frac{\sum_{i=1}^{n}(y_i - \hat{y}_i)^2}{\sum_{i=1}^{n}(y_i - \overline{y})^2} \tag{8}$$

where $\overline{y}$ is the mean of the actual fitness values. A higher R^2 value (closer to 1) suggests a better fit and higher reliability of the surrogate model.

The parameter settings for the optimization algorithm during testing are as follows: population size is set to 200, maximum number of iterations is 200, and the dimension of the test functions is 8. The algorithm parameters σ_0 is set as 0.2 and β is set as 0.8. Additionally, the neural network undergoes retraining at intervals of every five generations. The results are shown in Figures 1–3, which demonstrate that the algorithm is capable of converging to the minimum values and the surrogate model maintains a low RMSE and a high R^2 score, demonstrating its reliability in predicting fitness values.

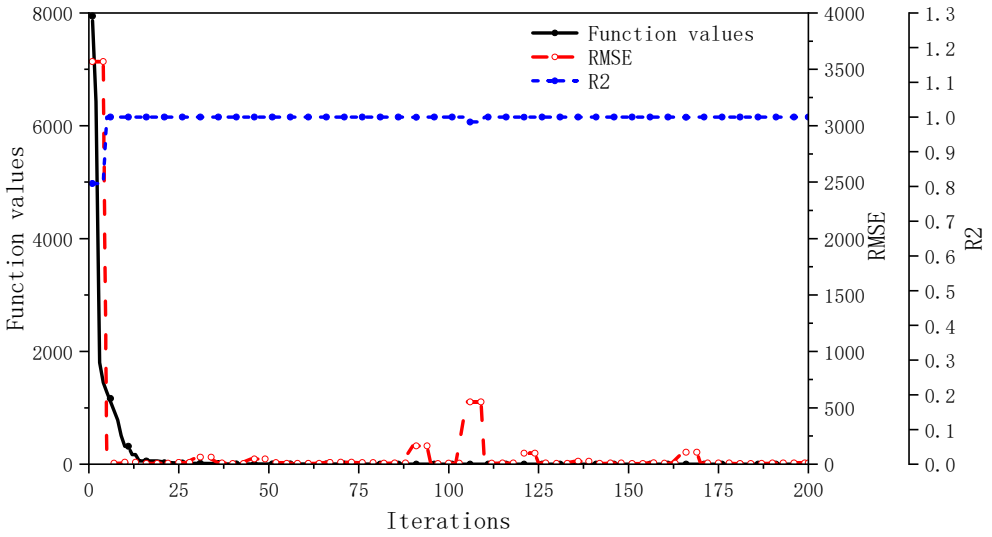


Figure 1. Results of the proposed algorithm on test function f1.

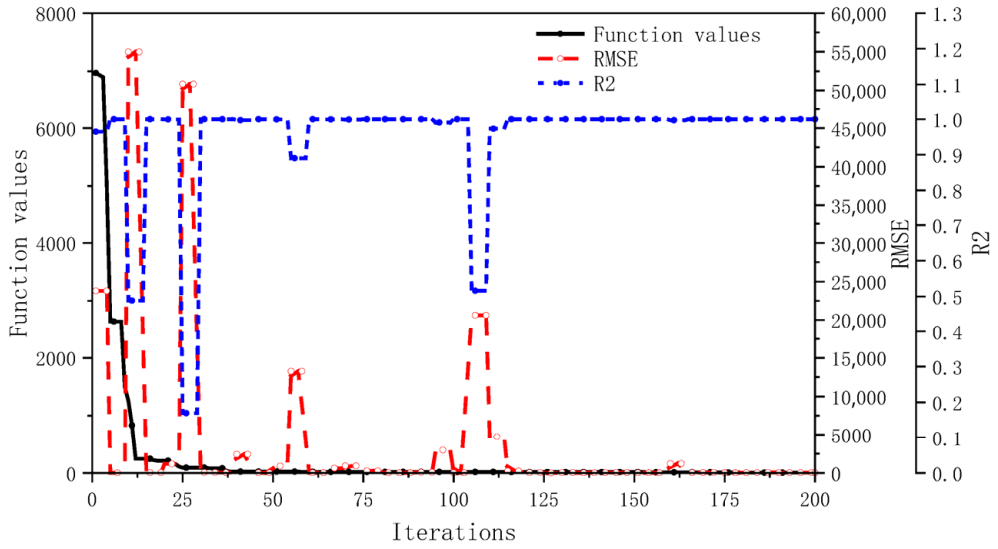


Figure 2. Results of the proposed algorithm on test function f2.

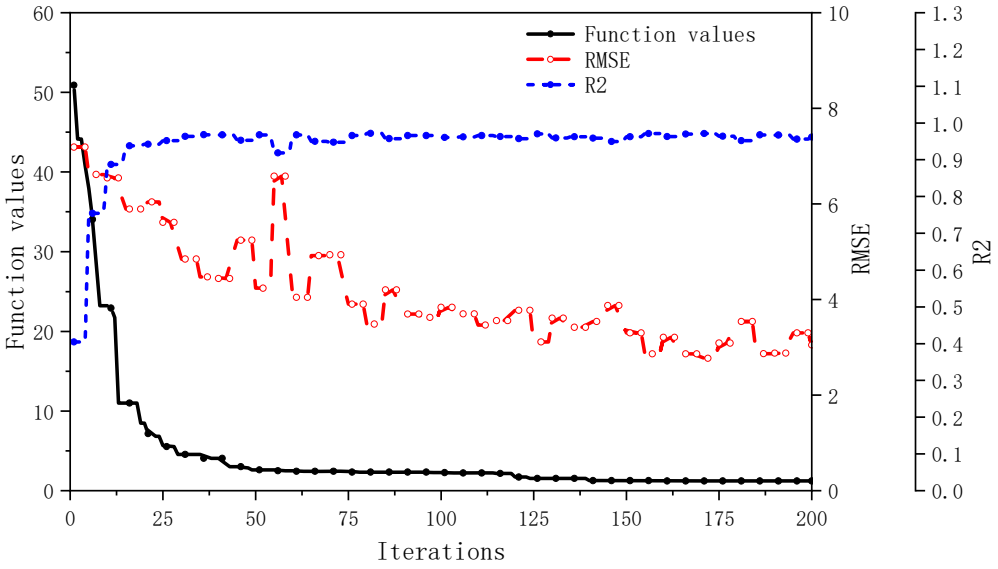


Figure 3. Results of the proposed algorithm on test function f3.

3. Design and Optimization

For the optimization and design of a high-efficiency broadband Doherty power amplifier, the design methodology is illustrated in the flowchart shown in Figure 4.

3. Objective Function Design

For the optimization and design of broadband power amplifiers, optimizing performance at a single frequency point is insufficient to meet the overall performance requirements. Therefore, applying a holistic approach to broadband power amplifier design is particularly important.

To address issues commonly found in traditional Doherty power amplifier designs—such as complex matching networks, potential efficiency degradation, and narrow operating bandwidth—this project proposes a novel design method. Specifically, a minimization-based approach is adopted for the design of the objective function. The core idea is as follows: if the maximum values of the various performance metrics within the operating bandwidth can be minimized while still satisfying the optimization goals, then the performance across the entire operating frequency range can also meet the desired specifications.

$$F_{P_out} = \frac{O_P_out}{min(P_out(f_{pi}))} \tag{9}$$

$$F_{DE_sat} = \frac{O_DE_sat}{min(DE_sat(f_{pi}))} \tag{10}$$

$$F_{Gain_sat} = \frac{O_Gain_sat}{min(Gain_sat(f_{pi}))} \tag{11}$$

$$F_{DE_6dB} = \frac{O_DE_6dB}{min(DE_6dB(f_{pi}))} \tag{12}$$

$$F_{Gain_6dB} = \frac{O_Gain_6dB}{min(Gain_6dB(f_{pi}))} \tag{13}$$

$$F_{Gain_30} = \frac{O_Gain_30}{min(Gain_30(f_{pi}))} \tag{14}$$

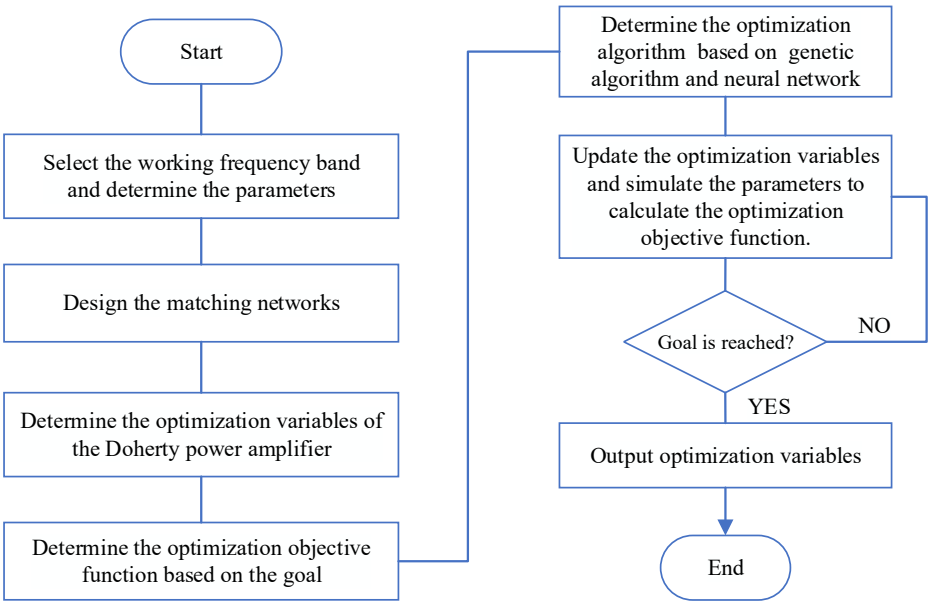


Figure 4. Flowchart of the design method for broadband Doherty power amplifiers.

The target values in the objective function are as follows: *O_P_out* is the target value of saturated power, *O_DE_sat* is the target value of saturated efficiency, *O_Gain_sat* is the target value of saturated gain, *O_DE_6dB* is the target value of 6 dB back-off efficiency, *O_Gain_6dB* is the target value of 6 dB back-off gain, and *O_Gain_*30 is the target value of gain at 30 dBm output power. $P_out(f_{pi})$ is the saturated output power at the design frequency point f_{pi}, $DE_sat(f_{pi})$ is the saturated efficiency at f_{pi}, $Gain_sat(f_{pi})$ is the saturated gain at f_{pi}, $DE_6dB(f_{pi})$ is the 6 dB back-off efficiency at f_{pi}, $Gain_6dB(f_{pi})$ is the 6 dB back-off gain at f_{pi}, and $Gain_30(f_{pi})$ is the gain at 30 dBm output power at f_{pi}, which can be obtained through simulation.

All the above objective functions are expected to be less than or equal to 1. According to the formula of the objective function, the function value can be less than or equal to 1 only when the minimum values of indicators such as power, efficiency, and gain reach or exceed the target values.

$$F = max(F_{p_out}, F_{DE_sat}, F_{Gain_sat}, F_{DE_6dB}, F_{Gain_6dB}, F_{Gain_30}) \tag{15}$$

The final objective function F is defined as the maximum value among the individual objective functions mentioned above. When the maximum value of these objective functions is less than or equal to 1, it implies that all other objective functions are also less than or equal to 1, and the corresponding performance metrics such as power, efficiency, and gain have reached or exceeded their respective target values.

4. Matching Network Design

For the broadband power amplifier, the optimized frequency range is 1.5 GHz to 2.6 GHz. The structural diagram of the high-efficiency broadband Doherty power amplifier (DPA) is shown in Figure 5.

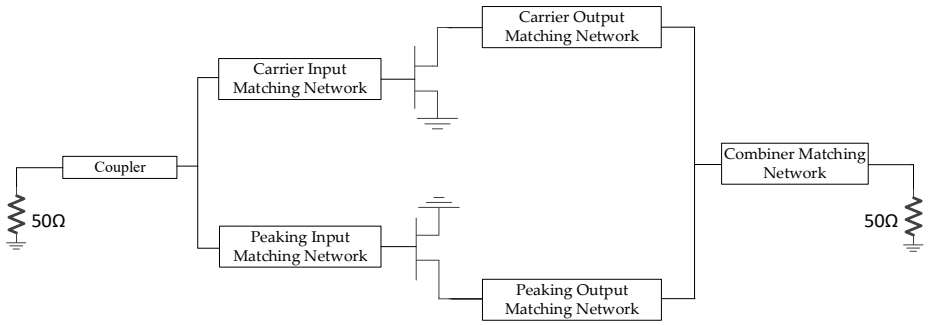


Figure 5. Schematic diagram of the high-efficiency broadband DPA structure.

The matching networks are composed of stepped-impedance matching sections, which are commonly employed in RF power amplifier design for their ability to achieve broadband impedance matching. The matching network for the carrier power amplifier is shown in Figures 6 and 7, while the matching network for the peaking power amplifier is illustrated in Figures 8 and 9. The combiner matching network structure is shown in Figure 10.

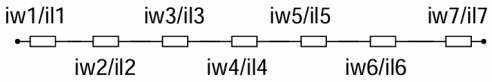


Figure 6. Carrier input matching network.

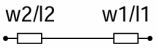


Figure 7. Carrier output matching network.

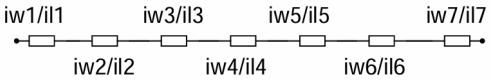


Figure 8. Peaking input matching network.

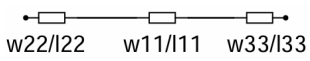


Figure 9. Peaking output matching network.

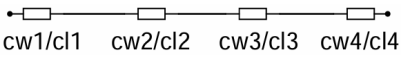


Figure 10. Combiner matching network.

5. Optimization of the DPA

This section focuses on the optimization design of the input matching network, output matching network, and combiner matching network of the high-efficiency broadband DPA, involving a total of 32 optimization variables.

To achieve high-efficiency broadband Doherty power amplifier optimization, a hybrid algorithm is applied to the design of the DPA operating in the 1.5 GHz to 2.6 GHz range. With a frequency step of 100 MHz, a total of 12 optimization frequency points are selected. For the DPA within the 1.5–2.6 GHz range, the optimization targets for efficiency, output power, and gain are listed in Table 2. When the minimum values of efficiency and output power across all frequency points in the band meet the optimization requirements, the overall power amplifier is considered to satisfy the design criteria.

Table 2. Optimization targets for the broadband power amplifier.

Performance Metrics	Optimization Target Values
P_out (dBm)	42
DE_sat (%)	50
DE_6dB (%)	45
Gain_sat (dB)	9
Gain_6dB (dB)	11
Gain_30 (dB)	12

The parameters for the optimization algorithm used in the process are set as follows: population size of 100, number of iterations of 100, initial mutation strength σ_0 set to 0.15, and β set to 0.5. Additionally, a penalty value is introduced—when the set targets are not met, the fitness value is significantly increased. This approach enhances diversity and benefits the neural network's prediction performance. The results are shown in Figure 11, where the improved algorithm reaches the optimization goals around the 75th generation.

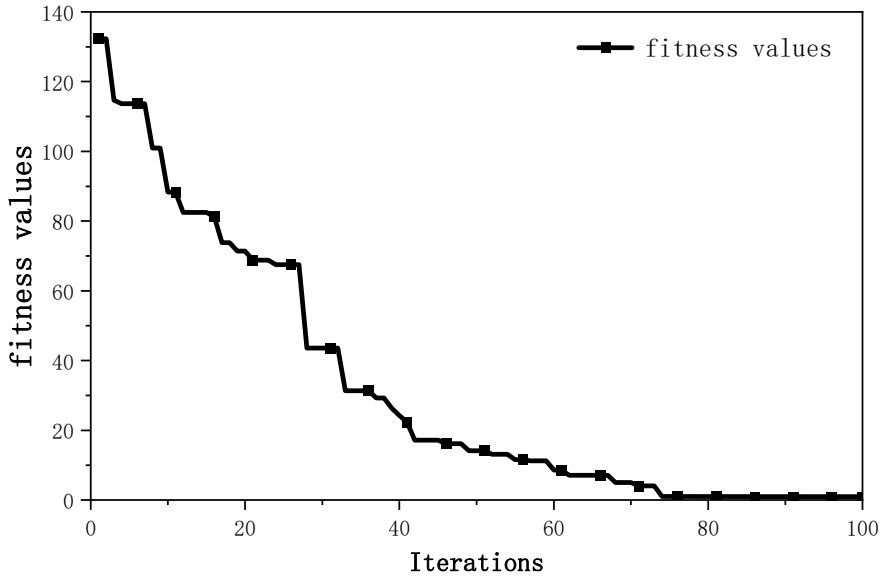


Figure 11. Fitness value curve of broadband PA optimization.

The optimal matching network parameters obtained from the optimization of the high-efficiency broadband DPA are listed in Table 3.

The complete schematic of the Doherty power amplifier is shown in Figure 12.

The optimized Doherty power amplifier was simulated, and the results are shown in Figure 13. From the simulation, it can be observed that the designed power amplifier achieves a saturated efficiency ranging from 52% to 65.3% across the entire bandwidth. The efficiency at 6 dB power back-off ranges from 47% to 57.1%, and the saturated output power varies between 42.3 dBm and 44.6 dBm.

Table 3. Optimal parameters of the high-efficiency broadband DPA.

Variable	Value (mm)	Variable	Value (mm)
iw1	4.0	l1	4.2
iw2	1.3	l2	4.7
iw3	2.4	w11	7.2
iw4	2.2	w22	1.4
iw5	10.0	w33	1.7
iw6	1.0	l11	4.2
iw7	18.2	l22	4.7
il1	1.1	l33	16.8
il2	14.3	cw1	3.3
il3	8.7	cw2	4.1
il4	13.4	cw3	1.7
il5	6.7	cw4	2.6
il6	2.7	cl1	9.8
il7	8.9	cl2	8.0
w1	7.2	cl3	6.5
w2	1.4	cl4	9.5

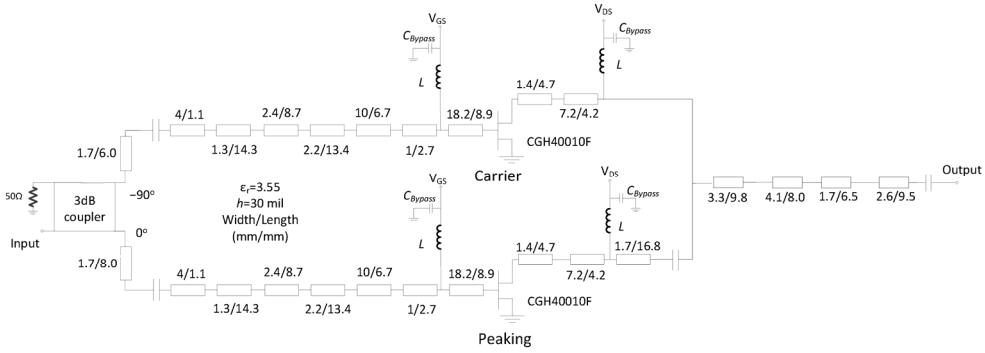


Figure 12. Complete schematic of the Doherty power amplifier.

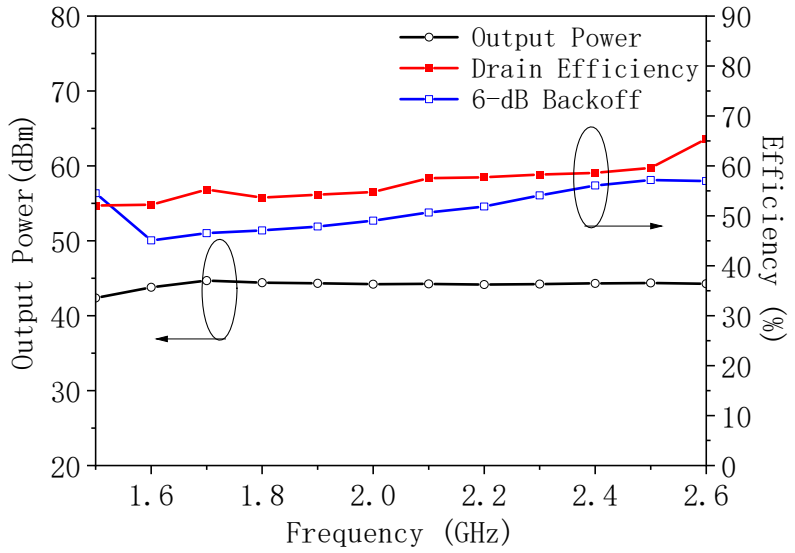


Figure 13. Simulation results of the Doherty power amplifier.

6. Algorithm comparison

This section focuses on the comparison between the GA and GA + NN algorithms. The algorithm parameters σ_0 is set as 0.15 and β is set as 0.5. The experimental platform

consists of an Intel 13900HX processor, an NVIDIA RTX 4060 Laptop GPU, 32 GB of RAM, ADS 2019 and MATLAB 2024a.

Firstly, the population size is set to 30 and maximum number of iterations is 50. The time required to execute the simulation is illustrated in Figure 14.

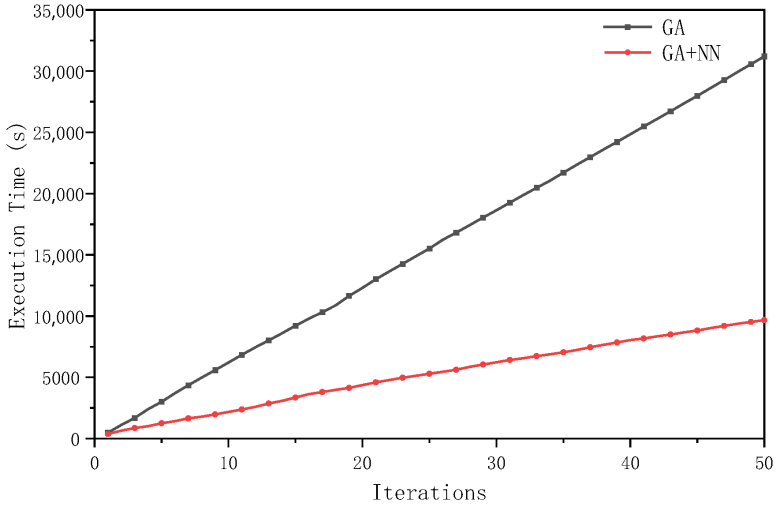


Figure 14. The time to execute simulation for the first time.

Secondly, the population size is set to 100 and the maximum number of iterations is 50. The time required to execute the simulation is illustrated in Figure 15.

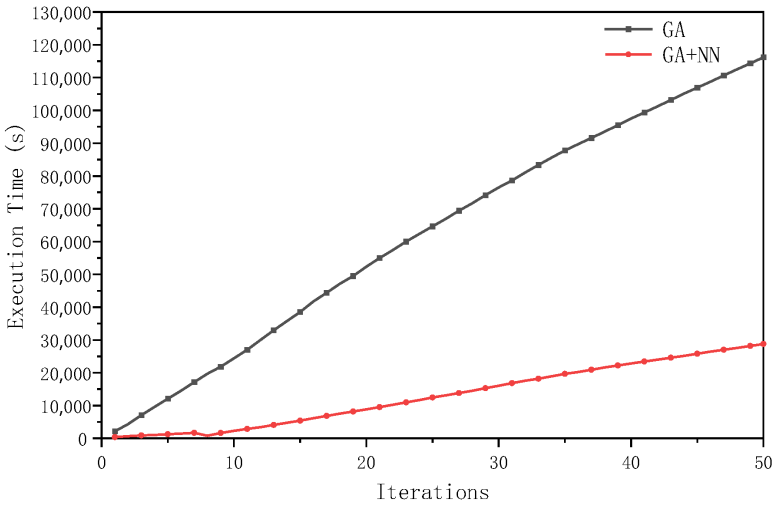


Figure 15. The time to execute simulation for the second time.

The comparative results of computational efficiency between the GA and GA + NN algorithms are presented in Table 4. For the 30 × 50 scale, the GA takes an average of 20.8 s to simulate one individual, whereas the GA + NN algorithm significantly reduces this time to 6.5 s. This represents a 68.7% reduction in simulation time when using GA + NN compared to GA. For the 100 × 50 scale, the GA requires an average of 23.2 s per simulation of one individual. In contrast, the GA + NN algorithm further decreases the simulation time to 5.8 s, indicating a 75% reduction compared to the GA. The integration of neural networks with genetic algorithms results in a substantial reduction in simulation time.

Table 4. Average time to execute simulation of one individual.

Algorithm Comparison	GA	GA + NN	Percentage
30 × 50	20.8 (s)	6.5 (s)	68.7%
100 × 50	23.2 (s)	5.8 (s)	75%

For the 100 × 50 scale, the fitness values of both algorithms exhibit a downward trend as the number of iterations increases, as shown in Figure 16. The overall performance difference between the two algorithms is not significant. Both algorithms are capable of converging to the optimal solution.

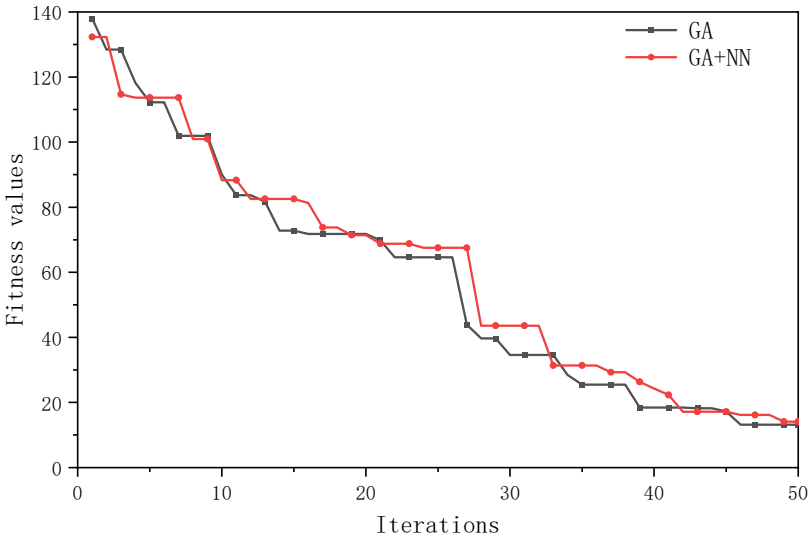


Figure 16. The comparison results of algorithm convergence.

4. Fabrication and Testing

To further verify the performance of the designed Doherty power amplifier, it was fabricated and tested. The testing environment and the fabricated prototype are shown in Figure 17. The prototype uses an RF35 dielectric substrate with a dielectric constant ε_r = 3.55 and a substrate thickness of h = 30 mil.

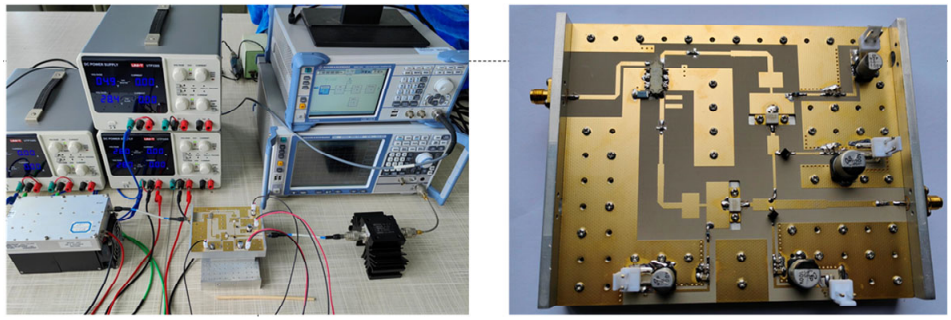


Figure 17. Testing environment and DPA: (**left**) testing environment; (**right**) high-efficiency broadband DPA.

The power and efficiency of the Doherty power amplifier were measured using a single-tone signal [20], with the results shown in Figure 18. As can be seen, across the entire operating bandwidth, the designed Doherty power amplifier achieves a saturated efficiency of approximately 51.4% to 61.8%, a 6 dB back-off efficiency of about 44.3 to 56.4% and a saturated output power ranging from 42.9 dBm to 44.7 dBm. The test results confirm that the designed Doherty power amplifier basically meets the design requirements.

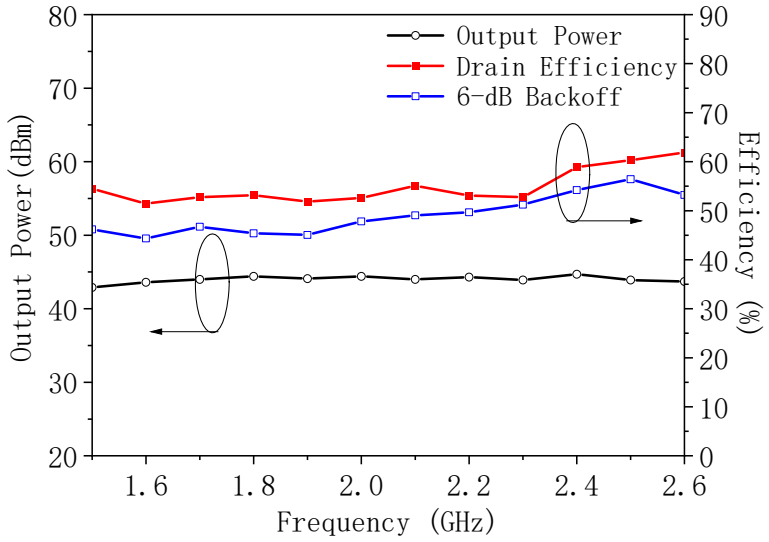


Figure 18. Power and efficiency test results at different frequencies.

The efficiency, gain, and output power of the Doherty power amplifier were tested at three frequency points: 1.5 GHz, 2.05 GHz, and 2.6 GHz. As shown in Figure 19, the saturated output power at all three frequencies exceeds 42 dBm, the gain is above 10 dB, and the saturated efficiencies are 54.5%, 56.6%, and 61.7%, respectively.

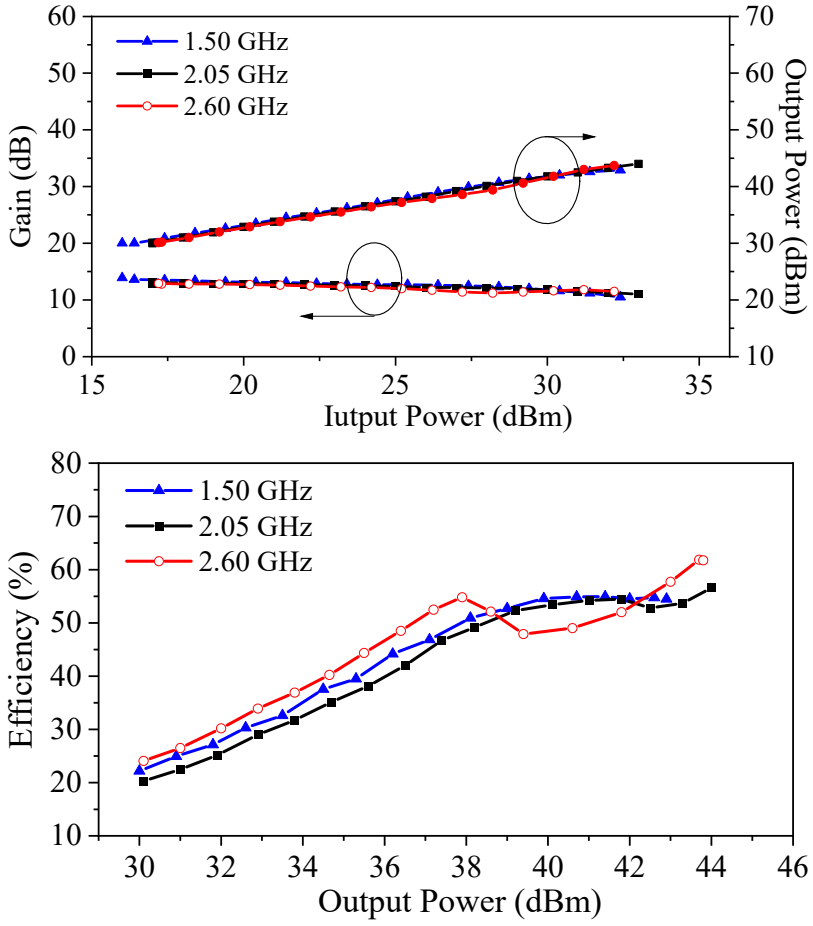


Figure 19. Test Results of the DPA: (**upper**) gain and output power; (**bottom**) efficiency variation with output power at different frequency points.

The comparison between the broadband power amplifier optimized in this work and related published studies is shown in Table 5. To facilitate a comprehensive comparison, we define a figure of merit as follows:

$$\mathrm{FOM} = \mathrm{BW} \times \mathrm{DE}_{\mathrm{SAT,avg}} \times \mathrm{DE}_{\mathrm{6dB,avg}} \tag{16}$$

where BW is the bandwidth, $\mathrm{DE}_{\mathrm{SAT,avg}}$ is the average saturation efficiency and $\mathrm{DE}_{\mathrm{6dB,avg}}$ is the average 6 dB efficiency.

Table 5. Performance comparison of power amplifiers.

Ref. (Year)	Freq. (GHz)	Pout@SAT (dBm)	DE@SAT (%)	DE@6dB (%)	Gain@SAT (dB)	FOM
[1] 2025	0.8–1.6	46–48	37–55 *	48–53	4–7 *	1858.4
[2] 2023	2.4–2.8	44.15–44.34	64.6–69.2	49.3–57.6	14 *	1430.3
[21] 2024	2.0–3.0	41.7–43.5	58.4–72.5	40.4–51.6	9.3–13.4	3665.2
[22] 2023	1.6–2.7	43.3–44.3	51–63	41–53	<8 *	2946.9
[23] 2023	1.3–2.1	50.3–53	28–62	42–53	-	1710
[24] 2024	1.3–2.0	43.9–44.3	60–70 *	52.0–65.8	10–14 *	2679.9
[25] 2018	1.45–2.35	44.3–46.8	58–70	47–60 *	7–10	3081.6
[26] 2016	1.5–2.5	42–44.5	55–75	42–53	8–10 *	3087.5
[27] 2015	1.7–2.6	44.6–46.3	57–66	47–57	10.2–11.6	2878.2
[28] 2013	1.5–2.4	>42 *	49–68	43–62	4–11 *	2764.1
This work	**1.5–2.6**	**42.9–44.7**	**51.4–61.8**	**44.3–56.4**	**10.5–11.3**	**3134.7**

*: Graphically estimated.

The results indicate that, while achieving comparable output power and efficiency, the design presented here attains a wider bandwidth. These optimization results validate the effectiveness of jointly optimizing the broadband power amplifier using the genetic algorithms and neural networks optimization algorithm.

5. Conclusions

This paper proposes a high-efficiency broadband Doherty power amplifier optimization design method based on a genetic algorithm combined with a neural network. A high-efficiency broadband Doherty power amplifier operating from 1.5 GHz to 2.6 GHz was designed. The test results demonstrate that the designed Doherty power amplifier achieves high saturated and back-off efficiencies within the operating bandwidth, while the output power meets the requirements, confirming the effectiveness and feasibility of the proposed method.

Author Contributions: Conceptualization, J.X. (Jianping Xing) and J.X. (Jing Xia); methodology, J.X. (Jianping Xing), Y.C. and Y.X.; software, J.X. (Jianping Xing) and Y.C.; validation, J.X. (Jianping Xing) and Y.X.; formal analysis, Y.C.; investigation, J.X. (Jianping Xing), Y.C. and Y.X.; resources, J.X. (Jing Xia); data curation, J.X. (Jianping Xing) and W.D.; writing—original draft preparation, J.X. (Jianping Xing); writing—review and editing, J.X. (Jing Xia); visualization, J.X. (Jianping Xing) and W.D.; supervision, J.X. (Jing Xia); project administration, J.X. (Jianping Xing); funding acquisition, J.X. (Jianping Xing). All authors have read and agreed to the published version of the manuscript.

Funding: This work was supported by the College Students' Innovative Entrepreneurial Training Plan Program 202410299196Y.

Institutional Review Board Statement: Not applicable.

Informed Consent Statement: Not applicable.

Data Availability Statement: The research data supporting this publication are available from the corresponding author upon reasonable request.

Conflicts of Interest: The authors declare no conflicts of interest.

References

1. Urvoy, J.B.; Quaglia, R.; Cripps, S.C. Design and simulation of a Doherty-mode OLMBA for enhanced back-off efficiency over an octave bandwidth. In Proceedings of the 2025 International Workshop on Integrated Nonlinear Microwave and Millimetre-Wave Circuits (INMMIC), Turin, Italy, 10–11 April 2025; pp. 1–4.
2. Wang, W.; Li, S.; Chen, S.; Cai, J.; Li, Y.; Zhou, X.; Crupi, G.; Wang, G.; Xue, Q. A broadband outphasing GaN power amplifier based on reconfigurable output combiner. *IEEE Trans. Microw. Theory Tech.* **2023**, *72*, 1030–1044. [CrossRef]
3. Xia, J.; Chen, W.; Meng, F.; Yu, C.; Zhu, X. Improved three-stage Doherty amplifier design with impedance compensation in load combiner for broadband applications. *IEEE Trans. Microw. Theory Tech.* **2018**, *67*, 778–786. [CrossRef]
4. Shahmoradi, M.; Javid-Hosseini, S.-H.; Nayyeri, V.; Giofrè, R.; Colantonio, P. A broadband Doherty power amplifier for sub-6GHz 5G applications. *IEEE Access* **2023**, *11*, 28771–28780. [CrossRef]
5. Wang, J.; Dai, Z.; Zhong, K.; Bai, G.; Bi, C.; Li, M.; Shi, W.; Pang, J. Design of a Dual-Band Doherty Power Amplifier Using Single-Loop Network. *IEEE Trans. Microw. Theory Tech.* **2024**, *72*, 5818–5829. [CrossRef]
6. Ni, Z.; Xia, J.; Zhou, X.; Kong, W.; Zhang, W.; Zhu, X. Design of a wideband symmetric large back-off range Doherty power amplifier based on impedance and phase hybrid optimization. *Front. Inf. Technol. Electron. Eng.* **2025**, *26*, 146–156. [CrossRef]
7. Chen, P.; Merrick, B.M.; Brazil, T.J. Bayesian Optimization for Broadband High-Efficiency Power Amplifier Designs. *IEEE Trans. Microw. Theory Tech.* **2015**, *63*, 4263–4272. [CrossRef]
8. Huang, J.; Fan, Z.; Cai, J. Design of a High-Efficiency Sequential Load Modulated Balanced Amplifier Based on Multiple Multiobjective Bayesian Optimization. *IEEE Trans. Comput. Aided Des. Integr. Circuits Syst.* **2024**, *43*, 4348–4360. [CrossRef]
9. Li, C.; You, F.; Yao, T.; Wang, J.; Shi, W.; Peng, J.; He, S. Simulated Annealing Particle Swarm Optimization for High-Efficiency Power Amplifier Design. *IEEE Trans. Microw. Theory Tech.* **2021**, *69*, 2494–2505. [CrossRef]
10. Liu, H.; Li, C.; He, S.; Shi, W.; Chen, Y.; Shi, W. Simulated Annealing Particle Swarm Optimization for a Dual-Input Broadband GaN Doherty Like Load-Modulated Balance Amplifier Design. *IEEE Trans. Circuits Syst. II Express Briefs* **2022**, *69*, 3734–3738. [CrossRef]
11. Ni, Z.; Xia, J.; Zhou, X.; Kong, W.; Zhang, H.; Yu, C.; Zhu, X.-W. Design and Analysis of Optimization Method for Ultra-Wideband PA Based on Improved MOEA/D Algorithm Using Mixed Objective Function. *IEEE Trans. Comput. Aided Des. Integr. Circuits Syst.* **2024**, *44*, 2641–2654. [CrossRef]
12. Liu, B.; Xue, L.; Fan, H.; Ding, Y.; Imran, M.; Wu, T. An Efficient and General Automated Power Amplifier Design Method Based on Surrogate Model Assisted Hybrid Optimization Technique. *IEEE Trans. Microw. Theory Tech.* **2024**, *73*, 926–937. [CrossRef]
13. Wang, J.; Li, J.; Wei, Y.; Meng, S.; Yang, T.; Wang, C. Inverse Design of Broadband Optimal Power Amplifiers Enabled by Deep Learning. *IEEE Trans. Microw. Theory Tech.* **2025**, 1–15. [CrossRef]
14. Rahmat-Samii, Y.; Werner, D.H. A Comprehensive Review of Optimization Techniques in Electromagnetics: Past, Present, and Future. *IEEE Trans. Antennas Propag.* **2025**, 1. [CrossRef]
15. Thakur, A.; Konde, A. Fundamentals of Neural Networks. *Int. J. Res. Appl. Sci. Eng. Technol.* **2021**, *9*, 407–426. [CrossRef]
16. Wang, P.; Ye, K.; Hao, X.; Wang, J. Handling shape optimization of superconducting cavities with DNMOGA. *Comput. Phys. Commun.* **2024**, *299*, 109136. [CrossRef]
17. Wang, P.; Ye, K.; Hao, X.; Wang, J. Combining multi-objective genetic algorithm and neural network dynamically for the complex optimization problems in physics. *Sci. Rep.* **2023**, *13*, 880. [CrossRef] [PubMed]
18. Roomi, F.F.; Vahedi, A.; Mirnikjoo, S. Multi-Objective Optimization of Permanent Magnet Synchronous Motor Based on Sensitivity Analysis and Latin Hypercube Sampling assisted NSGAII. In Proceedings of the 2021 12th Power Electronics, Drive Systems, and Technologies Conference (PEDSTC), Tabriz, Iran, 2–4 February 2021; pp. 1–5. [CrossRef]
19. Dongare, A.D.; Kharde, R.R.; Kachare, A.D. Introduction to artificial neural network. *Int. J. Eng. Innov. Technol.* **2012**, *2*, 189–194.
20. Zhang, H.; Xia, J.; Zhou, X.Y.; Ni, Z.; Kong, W.; Ge, X. Optimization Design of Irregular Broadband Doherty Power Amplifier Based on 3-Port Output Combining Network. In Proceedings of the 2024 IEEE MTT-S International Wireless Symposium (IWS), Beijing, China, 16–19 May 2024; pp. 1–3.
21. Duan, C.; Yuan, D.; Diao, Y. 2~3GHz Broadband Doherty Power Amplifier Based on Improved Carrier Power Amplifier Output Matching. In Proceedings of the 2024 IEEE MTT-S International Microwave Workshop Series on Advanced Materials and Processes for RF and THz Applications (IMWS-AMP), Nanjing, China, 9–11 November 2024; pp. 1–3.
22. Zhou, H.; Chang, H.; Fager, C. Symmetrical Doherty power amplifier with high efficiency and extended bandwidth. In Proceedings of the 2023 International Workshop on Integrated Nonlinear Microwave and Millimetre-Wave Circuits (INMMIC), Aveiro, Portugal, 8–11 November 2023; pp. 1–3.
23. Belchior, C.; Nunes, L.C.; Cabral, P.M.; Pedro, J.C. Sequential LMBA design technique for improved bandwidth considering the balanced amplifiers off-state impedance. *IEEE Trans. Microw. Theory Tech.* **2023**, *71*, 3629–3643. [CrossRef]

24. Zheng, Y.; Roblin, P. Bandwidth-enhanced mixed-mode outphasing power amplifiers based on the analytic role-exchange Doherty-chireix continuum theory. *IEEE Trans. Circuits Syst. I Regul. Pap.* **2024**, *71*, 3584–3596. [CrossRef]
25. Liu, G.; Cheng, Z.; Zhang, M.; Chen, S.; Gao, S. Bandwidth Enhancement of Three-device Doherty Power Amplifier based on Symmetric Devices. *IEICE Electron. Express* **2018**, *15*, 20171222. [CrossRef]
26. Chen, S.; Wang, G.; Cheng, Z.; Xue, Q. A Bandwidth Enhanced Doherty Power Amplifier With a Compact Output Combiner. *IEEE Microw. Wirel. Components Lett.* **2016**, *26*, 434–436. [CrossRef]
27. Pang, J.; He, S.; Huang, C.; Dai, Z.; Peng, J.; You, F. A Post-Matching Doherty Power Amplifier Employing Low-Order Impedance Inverters for Broadband Applications. *IEEE Trans. Microw. Theory Tech.* **2015**, *63*, 4061–4071. [CrossRef]
28. Gustafsson, D.; Andersson, C.M.; Fager, C. A Modified Doherty Power Amplifier With Extended Bandwidth and Reconfigurable Efficiency. *IEEE Trans. Microw. Theory Tech.* **2013**, *61*, 533–542. [CrossRef]

Disclaimer/Publisher's Note: The statements, opinions and data contained in all publications are solely those of the individual author(s) and contributor(s) and not of MDPI and/or the editor(s). MDPI and/or the editor(s) disclaim responsibility for any injury to people or property resulting from any ideas, methods, instructions or products referred to in the content.